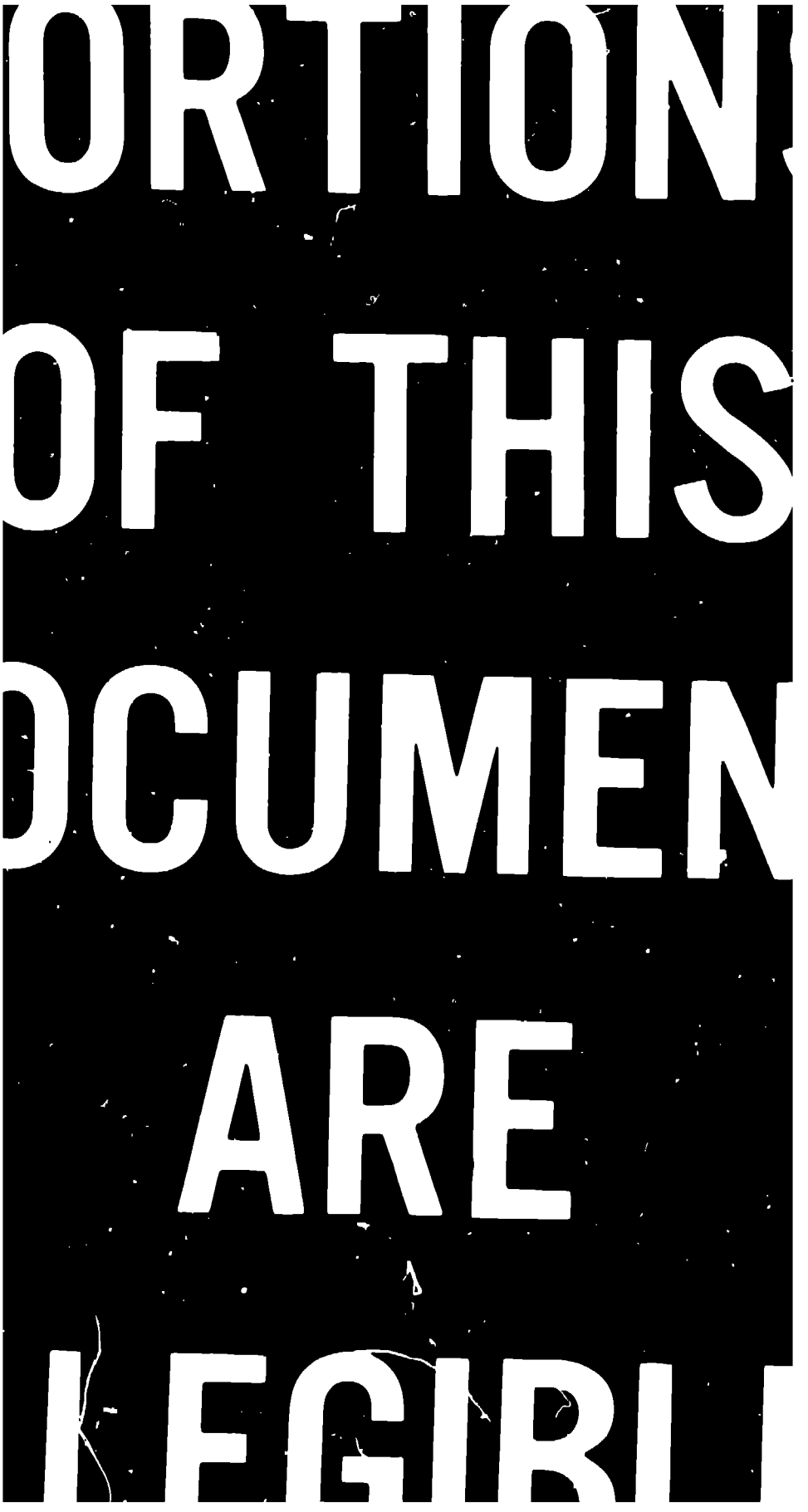
ORTION
OF THIS
DCUMEN
ARE
LEGIBL

CONF-810602--12

LA-UR-81-695

TITLE: NUMERICAL MODELING OF SHOCK-SENSITIVITY EXPERIMENTS

MASTER

AUTHOR(S): Allen L. Bowman, Charles A. Forest, James D. Kershner, Charles L. Mader, and George H. Pimbley

SUBMITTED TO: 7th Symposium (International) on Detonation

University of California

LOS ALAMOS SCIENTIFIC LABORATORY
Post Office Box 1663 Los Alamos, New Mexico 87545
An Affirmative Action/Equal Opportunity Employer

Form No. 836 R3
St. No. 2629
12/78

UNITED STATES
DEPARTMENT OF ENERGY
CONTRACT W-7405-ENG. 36

NUMERICAL MODELING OF SHOCK-SENSITIVITY EXPERIMENTS

Allen L. Bowman, Charles A. Forest, James D. Kershner,
Charles L. Mader, and George H. Pimbley
Los Alamos National Laboratory
Los Alamos, New Mexico

The Forest Fire rate model of shock initiation of heterogeneous explosives has been used to study several experiments commonly performed to measure the sensitivity of explosives to shock and to study initiation by explosive-formed jets. The minimum priming charge test, the gap test, the shotgun test, sympathetic detonation, and jet initiation have been modeled numerically using the Forest Fire rate in the reactive hydrodynamic codes SIN and 2DE.

INTRODUCTION

The Forest Fire rate model (1) of shock initiation of heterogeneous explosives has been used to describe the buildup to a propagating detonation, the passage of a detonation wave around a corner and along surfaces, the wave curvature , and the failure diameter (2). The Forest Fire model has now been used to study several experiments commonly performed to measure the sensitivity of explosives to shock and to study initiation by explosive-formed jets. The minimum priming charge test (3) has been modeled with the one-dimensional reactive hydrodynamic code SIN (4,5) and Forest Fire burn rate. The card gap test (6), the shotgun test, sympathetic detonation (7), and jet initiation (8) have been modeled with the two-dimensional code 2DE (4,9) and Forest Fire rates.

MINIMUM PRIMING CHARGE TEST

The minimum priming charge test assembly used at Los Alamos National Laboratory is shown in Fig. 1 (10). The test charge is a 2-in.-diam. by 2-in.-high cylinder. The Extex booster (a putty-like explosive of 80% PETN, 20% Sylgard 182) is placed in a hemispherical cavity milled in the center of the top of the cylinder. The cylinder and Extex are covered by a ½-in.-thick, 2-in.-diam. cylindrical brass plate that confines the explosive reaction. An MDF detonating fuse passes through the center of the brass plate to a detonator. The bottom of the test charge rests on a steel witness plate. The radius of the hemispherical cavity, and thus the mass of Extex booster explosive, are varied to find that radius at which 50% of the test trials result in detonation.

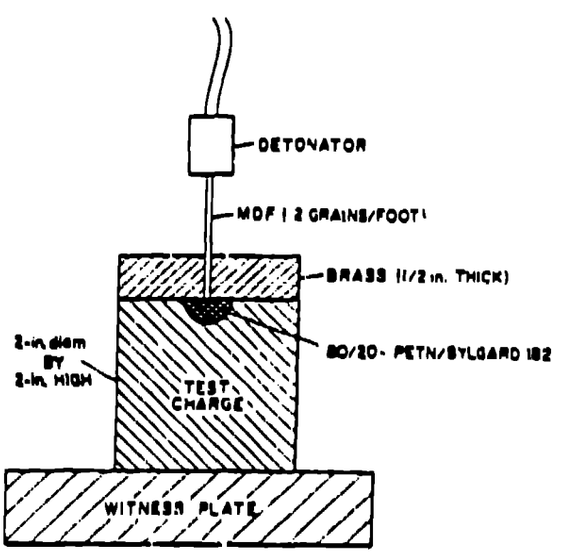

Fig. 1 - Minimum priming charge test assembly.

The minimum priming charge test was modeled using spherical symmetry. The spherical Extex booster charge is initiated by a 0.5-mm-radius hot spot at the center. The hot spot is defined as a region of completely reacted Extex (Extex detonation products) with density ρ and internal energy I at CJ conditions. The surrounding Extex is started with ρ_0 = 1.53 g/cm³ and I_0 = 0. The detonation through the Extex was calculated with the SIN option of C-J volume burn. A gamma-law isentrope for the Extex detonation products, with γ = 3.0 and an experimental detonation velocity of 7.26 mm/μs, was chosen as giving the best agreement with experiment. The results were found to be very sensitive to this choice.

Decomposition in the test charge (assumed to be a spherical shell around the booster) was modeled with Forest Fire rates derived from experimental Pop plots for PBX 9404 (11) and Comp. B - Grade A (12). The calculated maximum shock pressures are shown in Fig. 2 for PBX 9404 and in Fig. 3 for Comp. B as a function of the radial shock position, for various booster radii. Note that in each figure there is a curve for an Extex radius at which the shock pressure continues to decrease, but such that the next larger Extex radius causes growth of the shock to detonation pressure (P > 30 GPa). This abrupt transition radius, or more properly radius interval, is compared with the experimental 50% point in Table I.

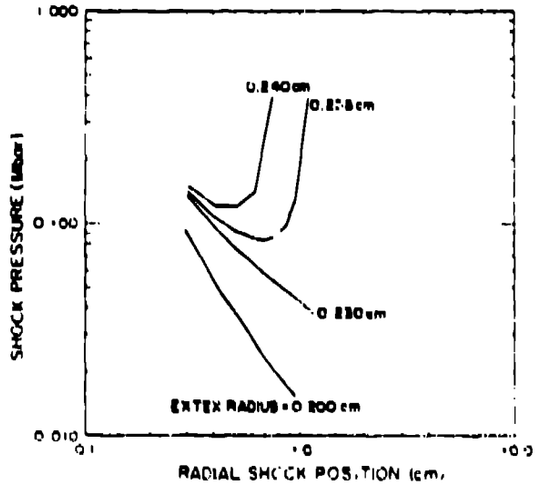

Fig. 2 Calculated maximum shock pressure as a function of shock position. The calculations used the γ = 3.0 Extex equation of state and the Forest Fire derived from the PBX 9404 lower bound Pop plot.

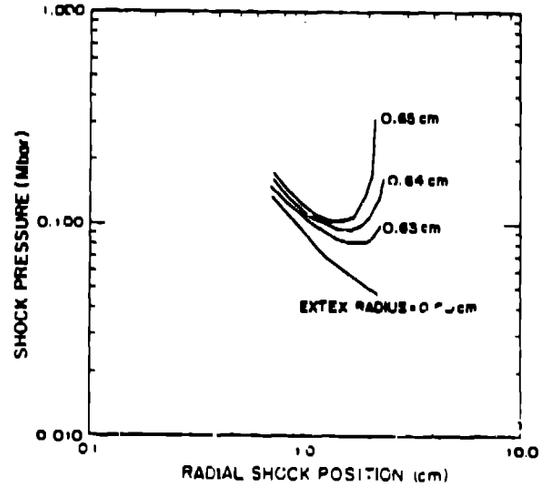

Fig. 3 - Calculated maximum shock pressure as a function of shock position. The calculations used the γ = 3.0 Extex equation of state and the Forest Fire derived from the Trott and Jung Comp. B-Grade A Pop plot.

TABLE I
Experimental and Calculated Results for the Minimum Priming Charge Test

	Extex Hemisphere Radius (mm)	
	Experiment 50% Point	Calculation Transition Interval
PBX 9404	1.95	2.30 - 2.35
Comp. B -	5.79	6.0 - 6.3

GAP TEST

The experimental arrangement of the Los Alamos standard, or large-scale, gap test is shown in Fig. 4 (10). The Dural spacer and relatively long booster are used to obtain greater precision in the tests. The gap length at which detonation of 50% of the samples would be expected to occur is estimated by the up and-down procedure. A 0.25-mm step height is used for the final determination of the 50% point. The NOL large-scale gap test (13) is shown in Fig. 5. A J-2 blasting cap (Hercules) is used to initiate the standard donor, which is

two pressed pentolite pellets with density of 1.56 g/cm³. The gap is made of Plexiglas (polymethyl methacrylate) disks and cellulose acetate cards. The test explosive is formed to fit a seamless steel tube with a 5.6-mm-thick wall. A 9.5-mm-thick mild steel witness plate is used. A "go" result is defined by a clean hole punched in the plate. The test procedure is a modification of the Bruceton up-and-down technique.

The gap tests were modeled with Forest Fire rates for all the explosives and propellants except pentolite. Because Pop plot data are not available to derive Forest Fire parameters for pentolite, the C-J volume burn model (4) was used for this explosive. The Plexiglas

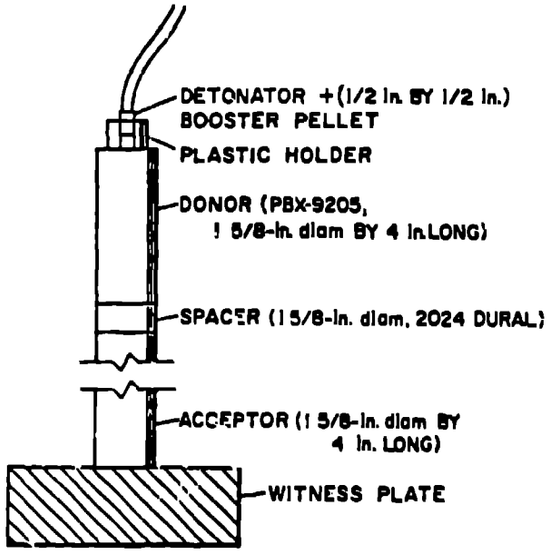

Fig. 4 - Los Alamos National Laboratory standard gap test assembly.

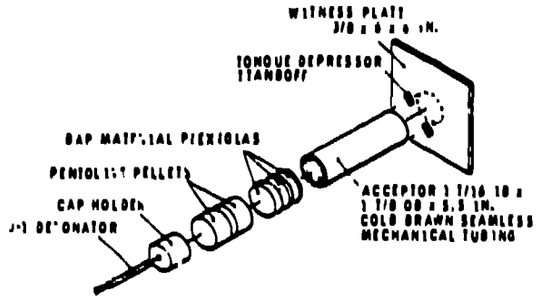

Fig. 5 - NOL large-scale gap test configuration.

was modeled with elastic-plastic flow, with shear modulus = 1.5 GPa, and yield strength = 0.5 GPa. Unconfined NOL gap test calculations were made with the same model, with the steel tube replaced by air. The Los Alamos test was initiated by a full-radius hot spot to model the effect of the ½-in. tetryl booster pellet. The NOL test was initiated by a hot spot of 3.7-mm radius and length to model the J-2 cap used by Hercules Inc.

The results of these calculations are summarized in Tables II and III. The poorest agreement between calculated and experimental results was obtained with Comp. B. This may be a consequence of the Pop plot that was used. The two available Pop plots for Comp. B are shown in Fig. 6 (12,14). The lower, more sensitive curve was used for these calculations. The upper curve would give a shorter critical gap length, probably less than the experimental value. The calibration of peak pressure in the gap (P_g) versus gap length (x) was obtained from these calculations. The calculated curve for the NOL gap test agrees with the published experimental curve (15) for x > 10 mm, and is better for shorter gap lengths. These results provide the first calibration for the Los Alamos test. The distances of run to detonation obtained from these calculations are plotted versus the induced pressure in Fig. 6 for comparison with the Pop plots obtained from wedge tests. The run distances from the gap tests are significantly longer than those from the wedge tests at induced pressures near the critical gap length values, but they approach each other at higher pressures. The critical run distance, i.e., the observed run distance at the critical gap length, clearly increases with increasing gap length in both types of gap tests.

SHOT GUN TEST

The shotgun test in its simplest form involves shooting a cylinder of explosive or high-energy rocket propellant from a shotgun at a target. The velocity of the sample is measured, and detonation is determined from the effect on the target. Hercules Inc. has developed an instrumented test facility, shown in schematic form in Fig. 7 (16), in order to study the entire process in detail.

The shotgun experiment was modeled with a cylinder of propellant, radius 6.5 mm and length 12.5 mm, making impact with a steel plate at a specified initial velocity. The calculation was

TABLE II
LOS ALAMOS STANDARD GAP TEST

	TATB		PBX 9404			
Gap (mm)	14.4	20.6	43.3	47.5	51.6	55.7
Pressures (GPa)						
Dural gap[a]	23.2	19.0	7.3	5.9	4.8	3.8
Induced in sample:						
Calculation	23.5	13.5	8.0	4.0	3.0	2.4
Impedance match	16.3	13.0	4.2	3.3	2.6	2.0
Run distance (mm)						
Pop plot	3	6	5	7	9	13
Calculation	7	--	4	8	19	--
Experimental 50% gap (mm)	21.9[b]		51.9 - 57.6[c]			

[a]Pressures from the calibration curve.

[b]Experimental sample had ρ = 1.870; calculation based on limited Pop plot data for material with ρ = 1.876.

[c]This range includes all separate observations for PBX 9404 with ρ > 1.84 (Ref. 10). Calculation based on ρ = 1.844.

TABLE III
NOL LARGE-SCALE GAP TEST

	VTQ-2			Composition B				
Gap (mm)	36.5	40.2	43.8	47.5	51.1	54.8	58.4	62.1
(in.)	1.44	1.58	1.73	1.87	2.01	2.16	2.30	2.44
Pressures (GPa)								
Plexiglas gap[d]	4.7	4.0	3.4	2.9	2.5	2.2	1.9	1.6
Induced in sample:								
Calculation	8.0	6.5	5.3	4.5	3.8	3.3	2.7	2.3
Impedance match	6.1	5.2	4.3	3.5	3.1	2.7	2.3	1.9
Run distance (mm)								
Pop plot	6	8	11	15	17	20	24	29
Calculation	11	22	--	19	27	40	69	--
Experimental 50% gap (in.)	1.60			2.01 - 2.18				
No confinement								
Run distance (calc.)	33	--						
Experimental 50% gap	1.50							

[d]Pressures from the calibration curve (Ref. 15).

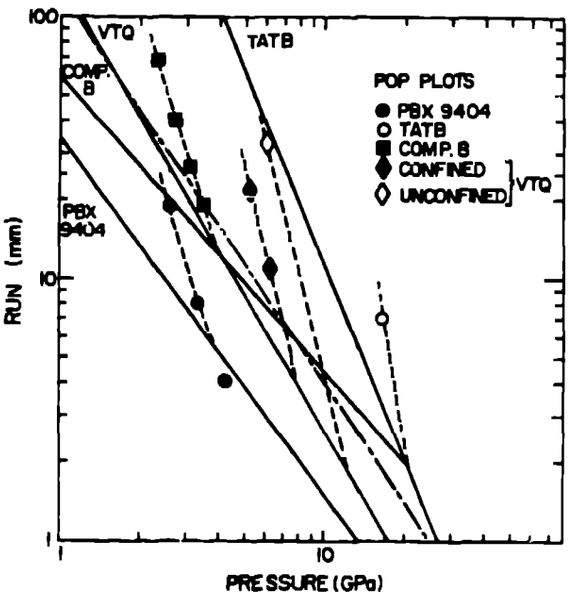

Fig. 6 - Pop plots of the test materials of this study, shown by solid lines. An alternate Pop plot for Composition B is shown by the dashed (- - -) line, indicating the degree of uncertainty in this material. The run-pressure points obtained from this study are plotted with two-dimensional Pop plots defined by the gap tests.

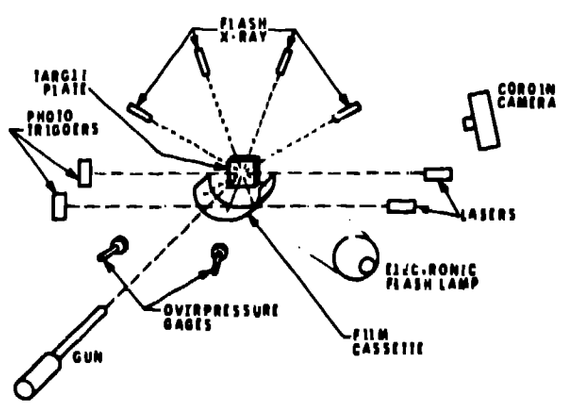

Fig. 7 - The instrumented shotgun test system.

started at the time of impact. The results are summarized in Table IV. The experimental minimum impact velocity for detonation of both these propellants is ∿0.7 mm/μs. The necessary condition for detonation appears to be that the run distance be less than the radius. The

TABLE IV
SUMMARY OF SHOTGUN RESULTS

Velocity (mm/μs)	Result	Initial Shock (GPa)	Run Distance (cm)
	VOP		
0.3	No reaction	1.5	4.4
0.6	Partial reaction	3.5	1.1
0.9	Detonation	6.0	0.5
	FKM		
0.6	No reaction	3.1	1.9
0.9	Detonation	5.2	0.6

The minimum velocity required for detonation is ∿0.7 mm/μs for both propellants.

run distance is obtained from the Pop plot using the initial shock pressure. This pressure is derived by matching the target Hugoniot with the propellant Hugoniot, reflected from the initial velocity.

SYMPATHETIC DETONATION

Hercules Inc. has performed an extensive experimental study of the sympathetic detonation of selected rocket propellants studying the effects of size, shape, damage, method of initiation, and other variables. The simplest test involves two cubes of propellant mounted as shown in Fig. 8. The donor cube is backed by a steel plate, and is initiated by a J-2 cap inserted through a hole in the plate. The extent of reaction of the acceptor cube is determined by the effect on a lead witness cylinder. The 2-in. cubes of the basic experiment were modeled by equivalent cylinders, 2.8678 cm in radius and 5.0738 cm long, with a 0.002% difference in volume and a 0.1% difference in surface area of the matched faces. The cap initiation was modeled by an initial hot spot 0.8824 cm in radius and length. The same model was extended to experiments with 1- and 3-in. cubes.

The critical separation distance is defined as the midpoint between the longest gap for which detonation occurs and the shortest gap for which no detonation is observed. It appears from

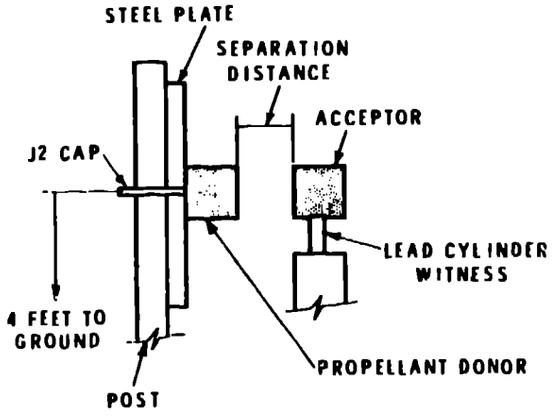

Fig. 8 - Schematic test setup for sympathetic detonation experiment. (4 ft. = 1.2192 m.)

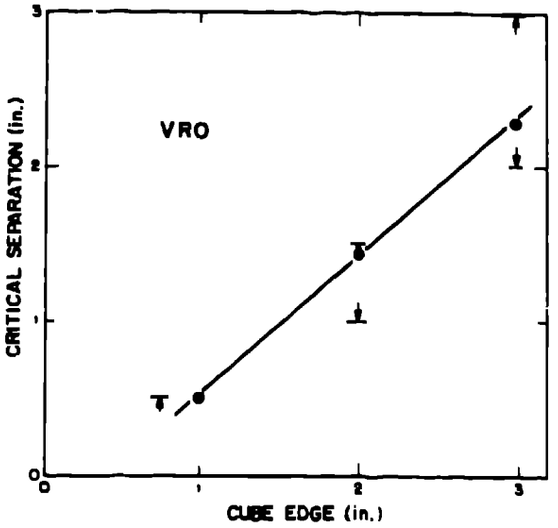

Fig. 9 - Variation of critical separation distance with cube size. Calculated values are shown by (•); experimental results are shown by arrows indicating the limits of observation.

comparison with experimental results that the critical separation distance represents the observed transition from high-order detonation to low-order detonation. Thus, a very significant reaction can be induced by a shock that is too weak to produce a direct shock-initiated detonation. This phenomenon was not investigated with our present model. The calculated critical separation distances for VRO cubes of different sizes are compared with experimental results in Fig. 9.

We can predict results from a consideration of run distances, blast wave pressures, and induced pressures in the acceptor. The necessary condition for detonation of the acceptor is that the length of run to detonation be less than approximately 0.75 times the radius of the acceptor. This run length is then converted to a necessary minimum induced pressure in the acceptor by means of the Pop plot. The blast pressure required to induce this pressure is obtained from

$$P_B = k p_i^{3/2} ,$$

with k = 0.02483 for VRO and the pressures in GPa. The distance from the donor at which this blast pressure will occur can be determined for the VRO cubes from Fig. 10. The effects on the blast pressure curves from varying L/d ratio, donor mass, method of initiation, and acceptor location have also been studied.

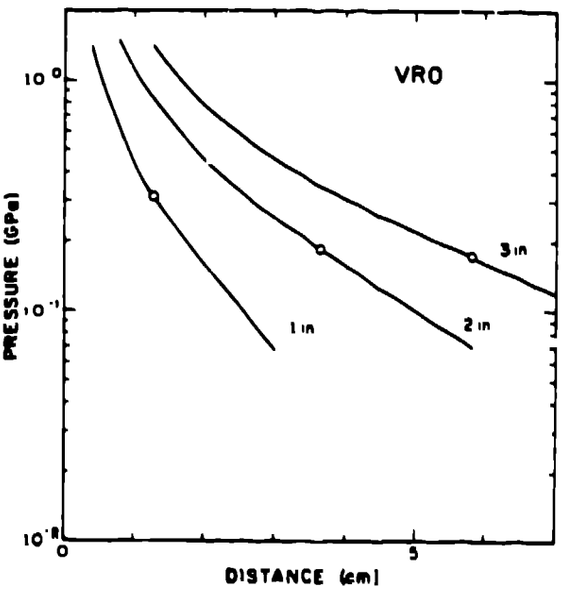

Fig. 10 - Variation of peak blast pressure with distance from the donor for three cube sizes. The critical separation distance is shown by (o).

JET INITIATION

The jet initiation of explosives has been studied by using shaped charges with copper cones to fire a copper jet into an explosive sample (17). The velocity was controlled by shooting the jet through a steel plate of appropriate thickness. The velocity and diameter of the jet were measured with velocity screens and flash x-ray photography. The critical jet parameter for initiation was found to be V^2d, where V is jet velocity and d is jet diameter.

This process was modeled by treating the jet as a solid cylinder with initial velocity V, starting the calculation at the time of impact. The results for copper jets fired into PBX 9404 and PBX 9502 are compared with experimental values of V^2d (18) in Table V. The jet initiates an overdriven detonation in PBX 9502 smaller than the critical diameter. This fails when it is decayed by side and rear rarefactions before it can expand beyond the critical diameter.

TABLE V
SUMMARY OF JET INITIATION WITH A COPPER JET

Diameter (mm)	Velocity (mm/μs)	Result	V^2d
PBX 9404: Experimental V^2d = 16			
2.0	2.0	Failed	8
2.0	2.5	Marginal	12.5
2.0	3.0	Propagated	18
4.0	2.0	Propagated	16
1.5	3.0	Marginal	13.5
PBX 9502: Experimental V^2d = 127			
4.0	5.0	Failed	100
4.0	6.0	Marginal	144
4.0	7.0	Propagated	196
8.0	4.0	Marginal	128
8.0	5.0	Propagated	200

CONCLUSIONS

The minimum priming charge test can be modeled fairly well in one-dimensional spherical geometry. The minimum detonation pressure is found to be ~6 GPa for PBX 9404 and ~7 GPa for Comp. B, indicating that this test is a high pressure, prompt shock initiation experiment. The gap test, shotgun test, and sympathetic detonation can be modeled with two-dimensional cylindrical geometry, and are shock initiation experiments with a sustained shock pulse. A detonation will occur when the shock wave is of sufficient strength and duration to build up to detonation. The shotgun and sympathetic detonation shock waves are planar across the face of the sample, resulting in pressure (p) versus run distance (x) in agreement with the Pop plot. The p-x condition for detonation is x > r (r is sample radius) for the shotgun test and x > 0.75r for sympathetic detonation, where the shock wave has some slight curvature. The gap test, on the other hand, shows p-x behavior very different from the Pop plot near the critical gap, as a consequence of the sharply curved shock wave that enters the sample. The process of shock initiation by a jet is in contrast with the other experiments. In a near-critical jet initiation, a prompt detonation of the explosive will occur. This will build to a propagating detonation only if the shock wave produced by the jet is of sufficient magnitude and duration.

REFERENCES

1. Charles A. Forest, "Burning and Detonation," Los Alamos Scientific Laboratory report LA-7245 (July 1978).

2. Charles L. Mader, "Two-Dimensional Homogeneous and Heterogeneous Detonation Wave Propagation," Sixth International Symposium on Detonation, ACR-221, 405 (1976).

3. Charles A. Forest, "Numerical Modeling of the Minimum Priming Charge Test," Los Alamos Scientific Laboratory report LA-8075 (1980).

4. C. L. Mader, Numerical Modeling of Detonations, University of California Press, Berkeley, 1979.

5. Charles L. Mader and Milton Samuel Shaw, "User's Manual for SIN," Los Alamos Scientific Laboratory report LA-7264-M (September 1978).

6. Allen L. Bowman, James D. Kershner, and Charles L. Mader, "A Numerical Model of the Gap Test," Los Alamos Scientific Laboratory report LA-8408 (1980).

7. Allen L. Bowman, James D. Kershner, and Charles L. Mader, "Numerical Modeling of Sympathetic Detonation," Los Alamos Scientific Laboratory report LA-7989 (1979).

8. C. L. Mader and G. H. Pimbley, "Jet Initiation of Explosives," Los Alamos Scientific Laboratory report LA-8647 (1981).

9. J. D. Kershner and C. L. Mader, "2DE, A Two-Dimensional Continuous Eulerian Hydrodynamic Code for Computing Multicomponent Reactive Hydrodynamic Problems," Los Alamos Scientific Laboratory report LA-4846 (March 1972).

10. M. J. Urizar, S. W. Peterson, and L. C. Smith, "Detonation Sensitivity Tests," Los Alamos Scientific Laboratory report LA-7193-MS (April 1978).

11. J. B. Ramsay and A. Popolato, "Analysis of Shock Wave and Initiation Data for Solid Explosives," in "Proc. 4th Symp. (Int.) on Detonation," White Oak, MD, Oct. 12-15, 1965, ONR report ACR-126 (1967), p. 233.

12. B. D. Trott and R. G. Jung, "Effect of Pulse Duration on Impact Sensitivity of Solid Explosives," in "Proc. 5th Symp. (Int.) on Detonation," Pasadena, CA, August 18-21, 1970, ONR report ACR-184 (1972), p. 191.

13. Donna Price, A. R. Clairmont, Jr., and J. O. Erkman, "The NOL Large Scale Gap Test. III. Compilation of Unclassified Data and Supplementary Information for Interpretation of Results," NOL report NOLTR 74-40 (March 1974).

14. John B. Ramsay, Los Alamos National Laboratory, unpublished data, 1963.

15. J. O. Erkman, D. J. Edwards, A. R. Clairmont, Jr., and Donna Price, "Calibration of the NOL Large Scale Gap Test: Hugoniot Data for Polymethyl Methacrylate," NOL report NOLTR 73-15 (April 1973).

16. R. C. Jensen, "Investigation of Impact-Initiated Detonations," 15th JANNAF Combustion Meeting, Newport, RI (Sept. 1978).

17. M. Held, "Initiating of Explosives, a Multiple Problem of the Physics of Detonation," Explosivstoffe 5, 98-113 (1968).

18. A. W. Campbell, Los Alamos National Laboratory, private communication (1980).